



Linkages Between the Great Arctic Cyclone of August 2012 and Tropopause Polar Vortices

Kevin Biernat*, Daniel Keyser, and Lance F. Bosart

Department of Atmospheric and Environmental Sciences,
University at Albany, SUNY

A43D-2478

*E-mail: kbiernat@albany.edu



1) Background

- Tropopause polar vortices (TPVs) are defined as tropopause-based vortices of high-latitude origin and are material features (Pyle et al. 2004; Cavallo and Hakim 2010)
- TPVs may interact with and strengthen jet streams, and act as precursors to the development of Arctic cyclones, including the Great Arctic Cyclone of August 2012 (hereafter AC12; e.g., Simmonds and Rudeva 2012; Yamazaki et al. 2015)
- Arctic cyclones may be associated with strong surface winds and poleward advection of warm, moist air, contributing to reductions in Arctic sea-ice extent (e.g., Zhang et al. 2013)
- Heavy precipitation, strong surface winds, and large waves due to Arctic cyclones may pose hazards to ships moving through open passageways in the Arctic Ocean
- AC12 was considered the "most extreme" Arctic cyclone in a 1979–2012 Climate Forecast System Reanalysis climatology of Arctic cyclones when considering a combination of factors, including minimum SLP, intensity, size, depth, and longevity (Simmonds and Rudeva 2012)
- AC12 led to reductions in Arctic sea-ice extent during a time in which Arctic sea ice was thin, with sea-ice volume decreasing twice as fast as normal during AC12 due to melting of bottom and perimeter ice floes (Zhang et al. 2013)
- Strong surface winds associated with AC12 helped to break up the thin Arctic sea ice as well (e.g., Parkinson and Comiso 2013)
- This study will examine the linkages between the development of AC12 and TPVs

2) Data and Methods

- Data: ERA-Interim (Dee et al. 2011)
- Utilized TPV tracking algorithm developed by Nicholas Szapiro and Steven Cavallo to identify and track TPVs of interest for AC12 (<https://github.com/nickszap/tpvTrack>)
- Manually tracked a predecessor surface cyclone (L1) and AC12 by following the locations of minimum SLP

3) Track and Intensity of TPVs and Cyclones

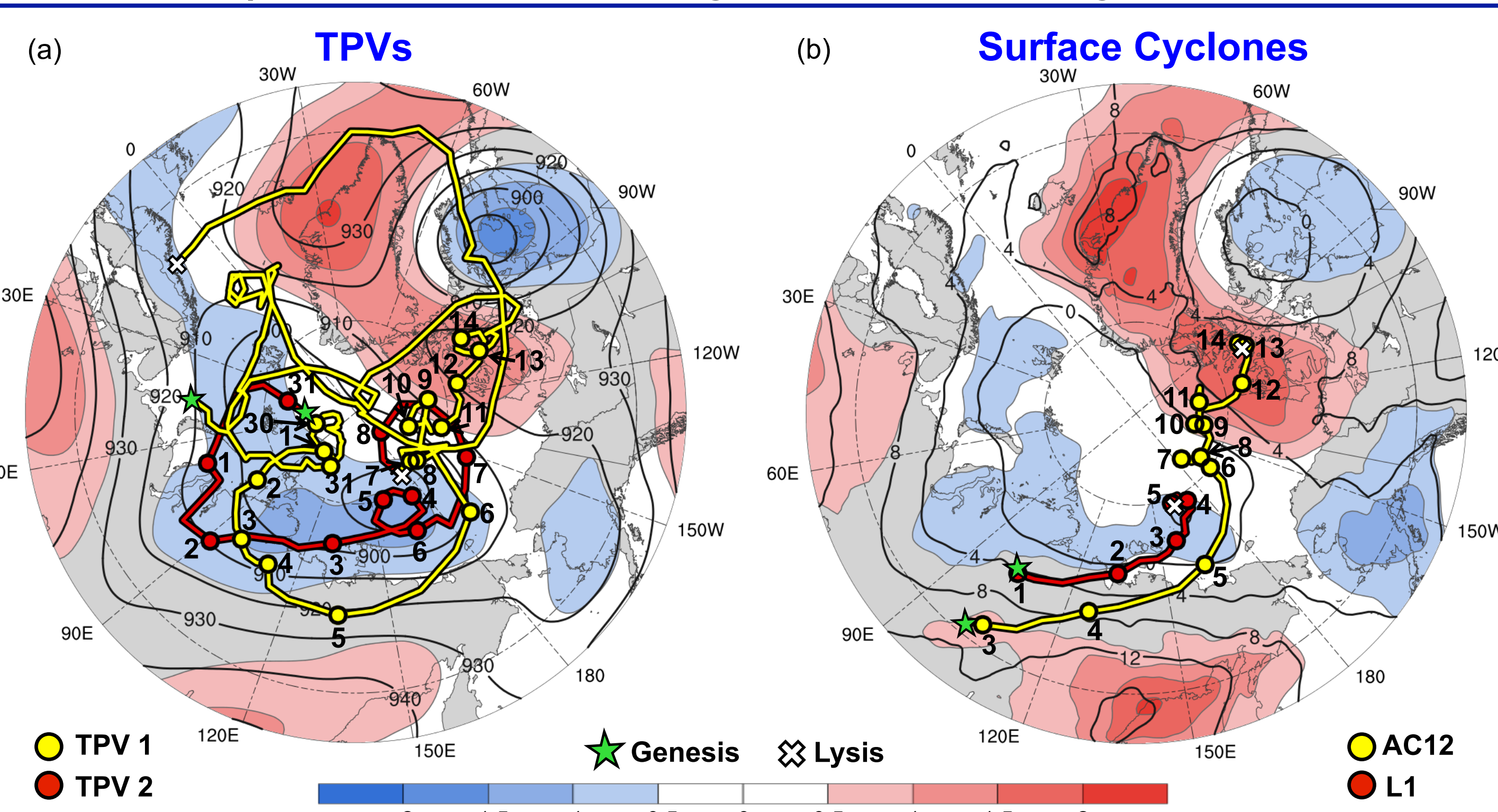


Figure 1. Total tracks of (a) TPV 1 (yellow line) and TPV 2 (red line), and (b) L1 (red line) and AC12 (yellow line) during respective lifetimes shown in Table 1. Dots correspond to 0000 UTC positions of the TPVs and surface cyclones during 30 July–14 August 2012, with the corresponding dates labeled. Also, 31 July–6 August 2012 time-mean (a) 300-hPa geopotential height (dam, dark gray) and standardized anomaly of 300-hPa geopotential height (σ , shaded), and (b) 850-hPa temperature ($^{\circ}\text{C}$, dark gray) and standardized anomaly of 850-hPa temperature (σ , shaded).

Feature	Date of Genesis	Date of Lysis	Lifetime (days)
TPV 1	23 Jul 2012	7 Sep 2012	~46
TPV 2	30 Jul 2012	8 Aug 2012	~9
L1	31 Jul 2012	5 Aug 2012	~5
AC12	2 Aug 2012	14 Aug 2012	~12

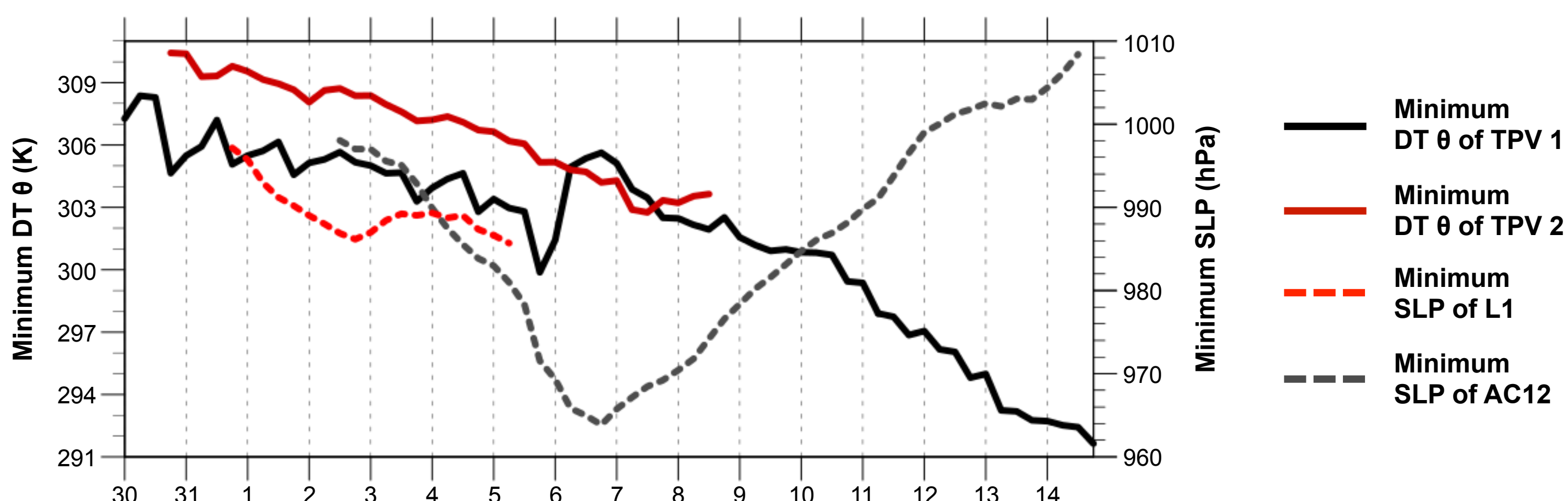


Figure 2. Time series of minimum dynamic tropopause (DT) potential temperature (θ) of TPV 1 (black, solid) and TPV 2 (red, solid), and minimum sea level pressure (SLP) of L1 (red, dashed) and AC12 (gray, dashed) during 30 July–14 August 2012.

4) Synoptic Evolution of TPVs and Cyclones

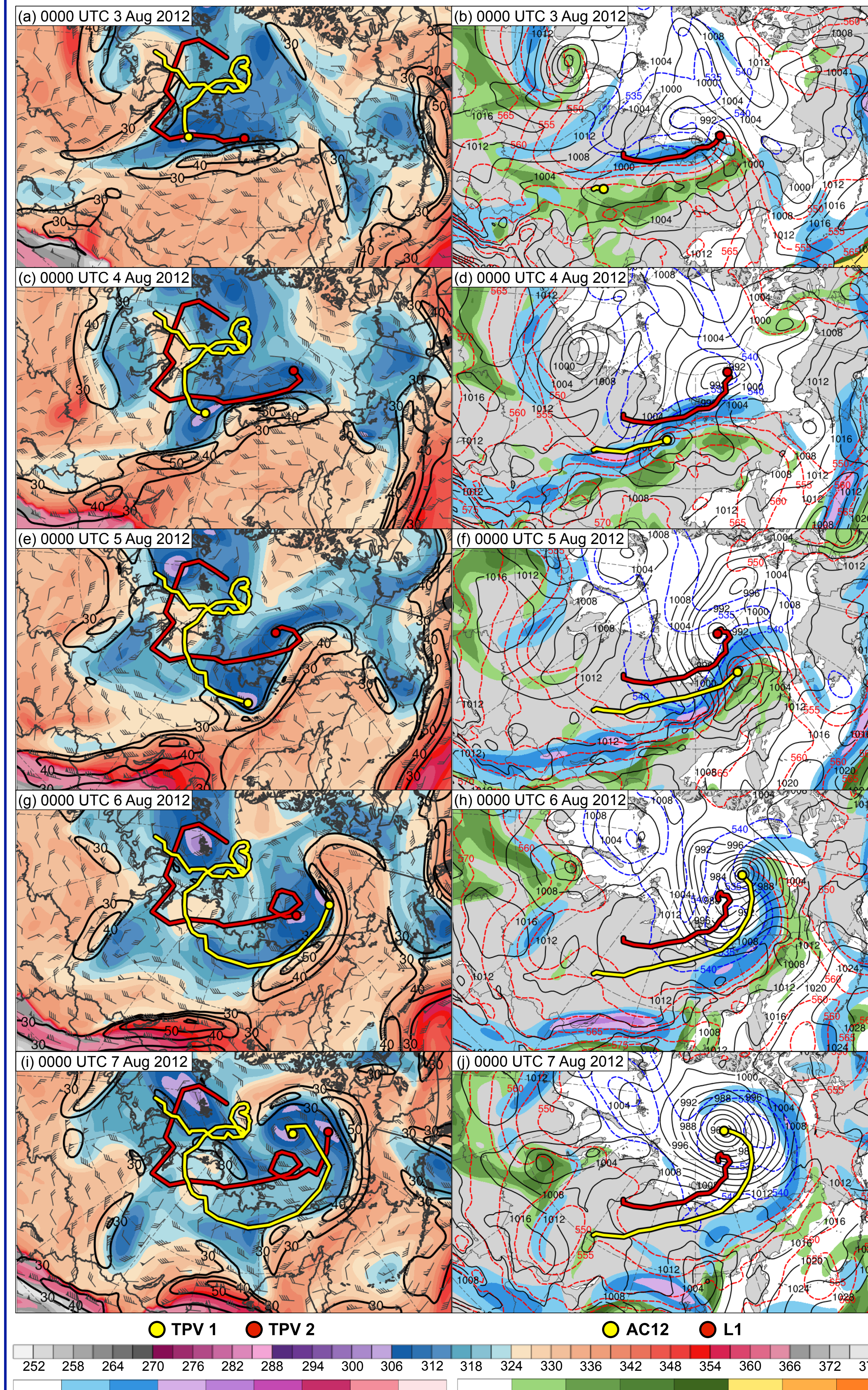


Figure 3. DT (2-PVU surface) θ (K, shading), wind speed (m s^{-1} , black), and wind (m s^{-1} , flags and barbs) at (a) 0000 UTC 3 August, (c) 0000 UTC 4 August, (e) 0000 UTC 5 August, (g) 0000 UTC 6 August, and (i) 0000 UTC 7 August 2012. 250-hPa wind speed (m s^{-1} , shading), 1000–500-hPa thickness (dam, dashed red and blue), SLP (hPa, black), and precipitable water (mm, shading) at (b) 0000 UTC 3 August, (d) 0000 UTC 4 August, (f) 0000 UTC 5 August, (h) 0000 UTC 6 August, and (j) 0000 UTC 7 August 2012.

References

- Cavallo, S. M., and G. J. Hakim, 2010: Composite structure of tropopause polar cyclones. *Mon. Wea. Rev.*, **138**, 3840–3857.
- Dee, D. P., and Coauthors, 2011: The ERA-Interim reanalysis: Configuration and performance of the data assimilation system. *Quart. J. Roy. Meteor. Soc.*, **137**, 553–597.
- Parkinson, C. L., and J. C. Comiso, 2013: On the 2012 record low Arctic sea ice cover: Combined impact of preconditioning and an August storm. *Geophys. Res. Lett.*, **40**, 1356–1361.
- Pyle, M. E., D. Keyser, and L. F. Bosart, 2004: A diagnostic study of jet streaks: Kinematic signatures and relationship to coherent tropopause disturbances. *Mon. Wea. Rev.*, **132**, 297–319.
- Simmonds, I., and I. Rudeva, 2012: The great Arctic cyclone of August 2012. *Geophys. Res. Lett.*, **39**, L23709.
- Yamazaki, A., J. Inoue, K. Dethloff, M. Maturilli, and G. König-Langlo, 2015: Impact of radiosonde observations on forecasting summertime Arctic cyclone formation. *J. Geophys. Res. Atmos.*, **120**, 3249–3273.
- Zhang, J., R. Lindsay, A. Schweiger, and M. Steele, 2013: The impact of an intense summer cyclone on 2012 Arctic sea ice retreat. *Geophys. Res. Lett.*, **40**, 720–726.

Acknowledgments

Special thanks to Nicholas Szapiro and Steven Cavallo for providing their TPV tracking algorithm. This research was supported by National Science Foundation Grant AGS-1355960.

5) Three-dimensional Structure of TPVs and Cyclones

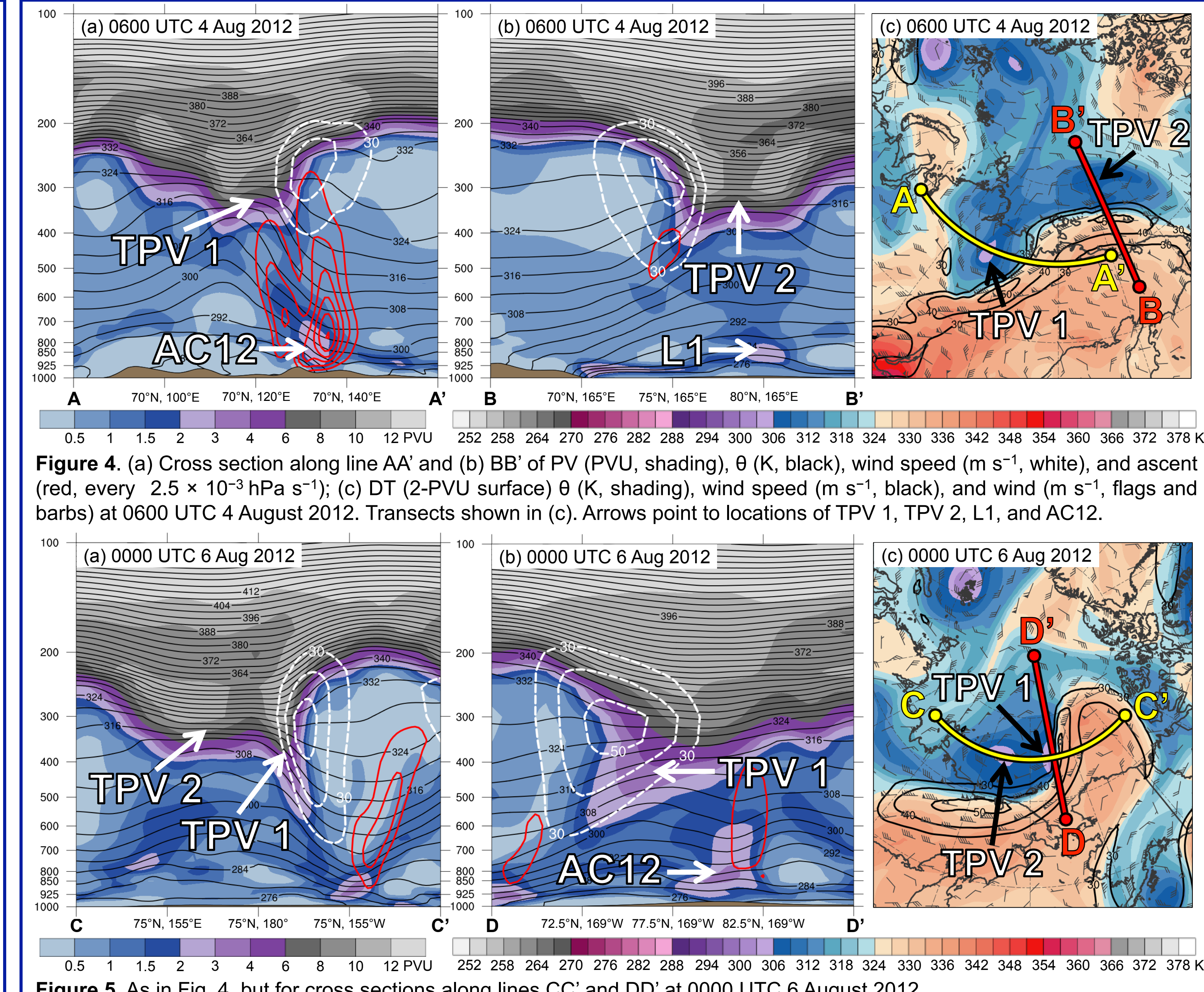


Figure 4. (a) Cross section along line AA' and (b) BB' of PV (PVU, shading), θ (K, black), wind speed (m s^{-1} , white), and ascent (red, every $2.5 \times 10^{-3} \text{ hPa s}^{-1}$); (c) DT (2-PVU surface) θ (K, shading), wind speed (m s^{-1} , black), and wind (m s^{-1} , flags and barbs) at 0600 UTC 4 August 2012. Transsects shown in (c). Arrows point to locations of TPV 1, TPV 2, L1, and AC12.

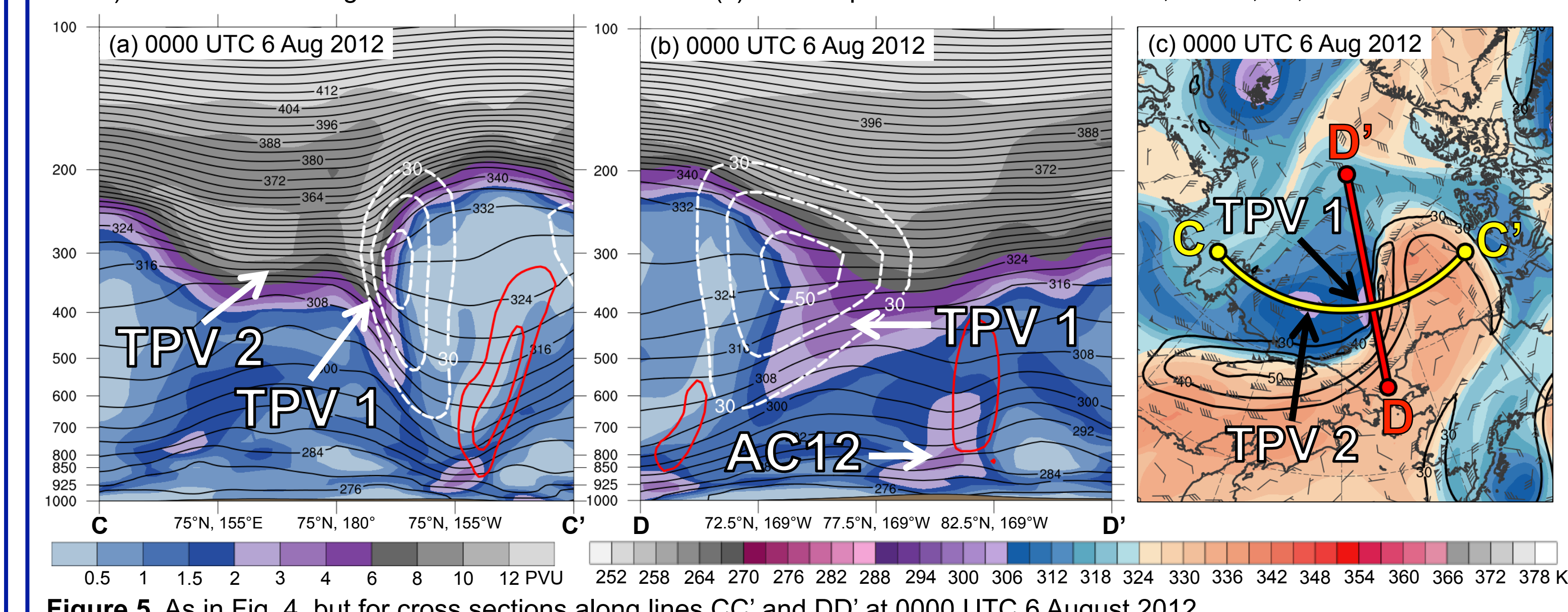


Figure 5. As in Fig. 4, but for cross sections along lines CC' and DD' at 0000 UTC 6 August 2012.

6) Impacts of Cyclones on Arctic Sea Ice

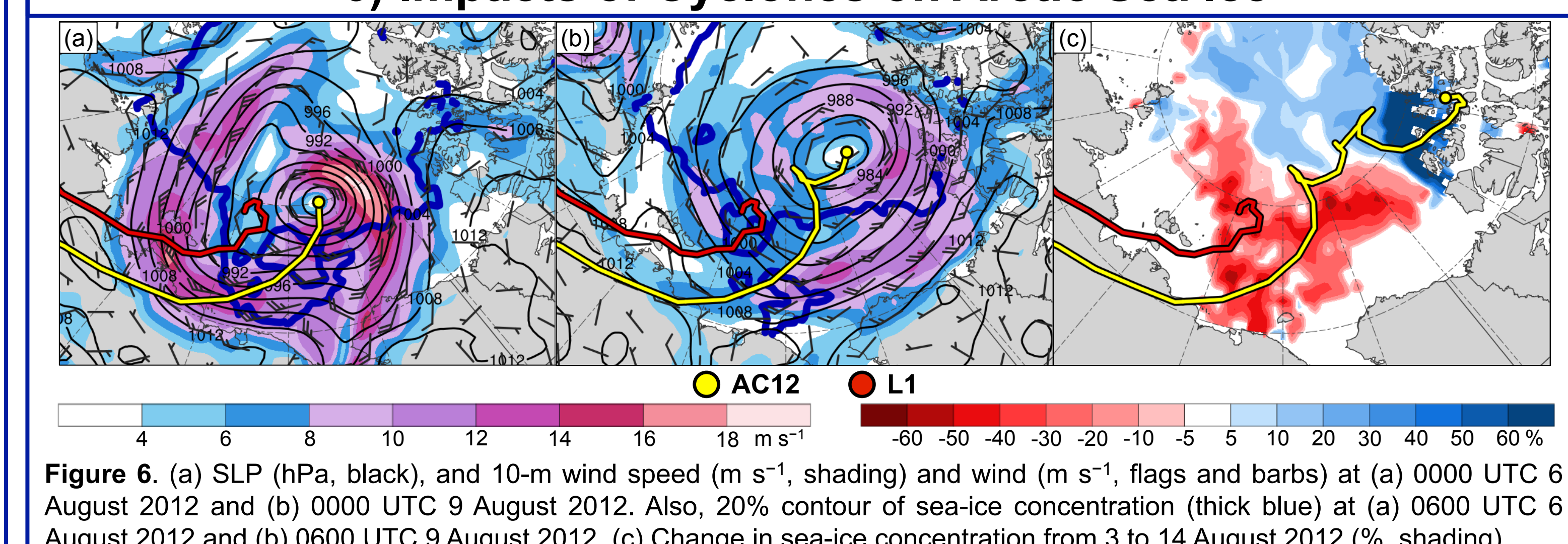


Figure 6. (a) SLP (hPa, black), and 10-m wind speed (m s^{-1} , shading) and wind (m s^{-1} , flags and barbs) at (a) 0000 UTC 6 August 2012 and (b) 0000 UTC 9 August 2012. Also, 20% contour of sea-ice concentration (thick blue) at (a) 0600 UTC 6 August 2012 and (b) 0600 UTC 9 August 2012. (c) Change in sea-ice concentration from 3 to 14 August 2012 (%), shading.

7) Discussion

- TPV 1 approaches and interacts with AC12 in region of strong baroclinicity (Figs. 1a,b and Figs. 3a–j), likely supporting the development of AC12 via baroclinic processes, consistent with previous studies (e.g., Simmonds and Rudeva 2012; Yamazaki et al. 2015)
- TPV–jet interactions involving both TPV 1 and TPV 2 (Fig. 3c and Figs. 4a–c) likely contribute to the formation of a dual-jet configuration and jet coupling over AC12 (Figs. 3c,d)
- Jet coupling and presence of warm, moist air (Figs. 3c,d) likely support relatively strong low-level ascent over AC12 (Fig. 4a), and TPV–jet interaction involving TPV 1 likely contributes to tropopause folding associated with TPV 1 (Figs. 5a–c)
 - Latent heating tied to the low-level ascent may contribute to an increase in magnitude of low-level PV associated with AC12 (compare Fig. 5b to Fig. 4a) and formation of a PV tower associated with AC12 (Fig. 5b), concomitant with the intensification of AC12
 - Tropopause folding associated with TPV 1 and formation of PV tower associated with AC12 suggest strong interaction between TPV 1 and AC12, which would support the intensification of AC12
- L1 interacts and merges with AC12, which may further support the intensification of AC12 (Figs. 3f,h)
- Interaction occurs between TPV 1 and TPV 2 (Figs. 3e,g,i), but the degree to which this interaction plays a role in the development of AC12 remains an open question
- Widespread strong surface winds associated with AC12 contribute to reduction in Arctic sea-ice extent (Figs. 6a–c), consistent with past studies (e.g., Zhang et al. 2013)